Tech Science Press

Cross-Tier Interference Mitigation in 3D HetNets for LTE and Wi-Fi Access

M. Rekha[1,*] and M. Bhuvaneswari[2]

[1]Department of Electronics and Communication Engineering, Dhanalakshmi Srinivasan Engineering College (Autonomous), Perambalur, 621212, Tamil Nadu, India
[2]Department of Electronics and Communication Engineering Anna University, BIT campus, Tiruchirappalli, 620024, Tamil Nadu, India
*Corresponding Author: M. Rekha. Email: rekha.m@dsengg.ac.in

Abstract: Due to the unprecedented rate of transformation in the field of wireless communication industry, there is a need to prioritise the coverage, network power and throughput as preconditions. In Heterogeneous Networks (HetNets) the low power node inclusion like Femto and Pico cells creates a network of Multi-Tier (M-Tier) which is regarded as the most significant strategy for enhancing the coverage, throughput, 4G Long Term Evolution (LTE) ability. This work mainly focuses on M-Tier 3D Heterogeneous Networks Energy Efficiency (EE) based Carrier Aggregation (CA) scheme for streaming real-time huge data like images. At first, M-Tier 3D HetNets scheme was made for investigating Signal to Noise Interference Ratio (SNIR) on assessing the collective Pico-tier and Femto-tier interference. Next, the scheme of channel allocation is scrutinised so as to estimate throughput from the multiple tiers. Additionally, with the use of CA technique, the problem of energy efficiency for M-Tier 3D Heterogeneous Network (HetNet) in relation to energy metrics and throughput was evaluated with the use of LTE and Wireless Fidelity (Wi-Fi) coexistence. The simulation is carried out in a MATLAB setting, and the outcomes reveal a huge impact on EE. The simulation is carried in terms of EE, transmission time, throughput, packet success rate, convergence probability, and coverage region. The analysis from simulation shows that on improving the output of the device, interference among small cell base stations is reduced on increasing EE. The outcomes attained aid in the effective creation of M-Tier 3D HetNets for enhancing EE by employing Multi-Stream Carrier Aggregation (MSCA) in HetNets.

Keywords: Heterogeneous networks; multi-tier 3D HetNets; energy efficiency; carrier aggregation; LTE; Wi-Fi

1 Introduction

Pico-cells, femto-cells, micro-cells, and Wi-Fi nodes, for example, are pursuing a major transformation from homogeneity to heterogeneity due to their rapid exploitation at low cost, and these lower power radio access nodes [1] function in both unlicensed and licensed spectra. Traditional cellular networks are overlaid

with a variety of Base Stations (BSs) such as femto-cells, pico-cells, and micro-cells, which aid in the realisation of views and the assistance of far higher data rates per unit than conventional networks. Every BS tier in heterogeneous cellular networks should have different features, such as different spatial density, path loss function, transmit power, and so on. How to classify interference and energy consumption from performance metrics like size, throughput, and coverage is a significant challenge in cellular HetNets deployment [2]. Interference control in HetNets must be evaluated and designed using tractable interference models and Energy-Efficient CA. However, in typical single-tier networks with BSs and a standard hexagonal grid in HetNets [3,4], with more topological diversity and randomness in each tier, energy efficient CA modelling has always been a difficult task.

Several researchers conducted a thorough investigation by taking into account various BS tiers in heterogeneous cellular networks [5] and modelling BS locations as a homogeneous poisson point mechanism. Some researchers proposed versatile User Equipment (UE) association scheme, in which each BS tier had different transmit capacity, spatial densities, and path loss exponents. With the widespread use of tablets and smartphones, cellular networks and higher data rates would be available everywhere and at any time. For example, Wi-Fi [6] is characterised by high peak data rates, but low efficiency for smaller packet sizes and limited coverage and is the major problem from the analysis of existing approaches [7]. As a result, the LTE network takes into account high spectral efficiency and widespread coverage. LTE small cells are being deployed as a supplement to LTE macro networks to address the need for increased cellular bandwidth. LTE networks must be supplemented with Wi-Fi access points (APs), and LTE cells must be installed separately from their surroundings in order to use unlicensed spectrum at 2.4 and 5 GHz. This might support the service providers and consumers by optimising data traffic [8,9].

There are some prevailing techniques in LTE/Wi-Fi HetNets that enable the user to access one or more concurrent radio interfaces for various applications [10]. When Wi-Fi appears to be available, for example, a user browsing the web can switch from LTE to Wi-Fi. In this case, a heterogeneous network can accommodate low latency and low bandwidth applications such as browsing over Wi-Fi and voice over IP on LTE at the same time. The policies communicated to users are currently network dependent or device dependent by managing the switching strategy across accessible access networks. Network discovery and selection functions collect policies, which are then transmitted to the client's computer. It is responsible for policy enforcement, i.e., appropriate interference selection based on network policy.

The minimization of latency and increasing of energy efficiency in LTE is possible through carrier aggregation. CA is a technology that combines one or more carriers to maximize data bandwidth. The primary goal of CA in Wi-Fi/LTE coexistence is to combine primary and secondary cells. This study aims to provide energy savings beyond federation bandwidth by using Wi-Fi interfaces and LTE at the same time. This can be accomplished by CA, which benefits the use of HetNets.

The combination of licensed and unlicensed spectrum aspects is explored in this inquiry, which is focused on background research and motivation. Three stages of network integration are seen here: 1) Create a multi-tier 3D HetNet model that interacts with applications such as multimedia data applications 2) Assessment of multi-stream carrier aggregation for better energy efficiency and optimum utilization of usable spectrum 3) In M-Tier HetNets, cross-tier interference is reduced by calculating the signal to noise interference ratio (SNIR). The aim of the research is to find a way to efficiently stream large amounts of data, such as images, between licensed and unlicensed spectrum. Both Wi-Fi and LTE networks have different Quality of Service (QoS) and data transmission rates, resulting in a large research gap in selecting a suitable HetNet model for data transmission over HetNet for combining LTE and Wi-Fi networks. This project aims to establish an effective network model for removing cross-tier interference, as well as an efficient distribution of higher data rates across licensed and unlicensed spectrum.

1.1 Contribution

The contribution of the proposed work has been summarized as: First, an M-Tier 3D HetNet model is developed. Unlike current methods, the proposed model uses 3D stochastic geometry to assess user position and BS with practical constraints in a multi-tier network. This work also examines cross-tier intervention in order to alleviate the active involvement of users' interference crisis. By combining licensed and unlicensed spectrum, this research work is expanded to deal with carrier aggregation for increased energy efficiency. In a suitable simulation environment, the output was evaluated and validated.

1.2 Organization

The work is arranged as follows: Section 2 discusses the current state of the HetNet model, Section 3 discusses the expected multi-tier 3D HetNet model, and Section 4 discusses carrier aggregation, which combines licensed and unlicensed spectrum. Section 4 contains the numerical findings with discussion, and Section 5 contains the conclusion and recommendations for future work.

2 Related Works

This section reviews the current literature on the relationship between the HetNet and the position of the CA in the HetNet context. LTE allows five bandwidth member carriers to converge and form a total bandwidth of 100 MHz. CA is accomplished by the use of a non-contiguous/contiguous channel stream.

Zhiyi Zhou et al. [2016] investigated spectrum allocation issues in HetNets using a variety of Radio Access Technologies (RATs) and average packet time as efficiency indicators [11]. Listen-before-talk queuing replicas for unlicensed bands are expected to sense reliability, lower spectral efficiency, and delay, similar to licensed bands. Spectrum allocation crisis is modelled as a bi-convex optimization problem using conservative approximation. Every RAT's spectrum is divided into k segments with the best solution. In comparison to traditional approaches such as maximum frequency reuse and orthogonal frequency reuse, Zhinyi Zhou demonstrated that the anticipated scheme provides an efficient traffic-aware spectrum allocation pattern that more efficiently utilises spectrum from each Rodent.

Mudassar Ali et al. [2018] expect optimal resource allocation for coexisting Wi-Fi and LTE-U networks in [12], with the aim of improving throughput and minimising interference. LTE-Unlicensed (LTE-U)/Wi-Fi resource distribution HetNets solves the optimization problem. Mesh Adaptive Direct Search (MADS) is expected to be a side effect of less-than-ideal performance. As LTE-U and LTE-L are combined, the simulation reveals that LTE-U outperforms Wi-Fi in terms of throughput. The MADS findings differ from the Outer Approximation Algorithm (OAA) findings. When MADS outperforms OAA, the computational complexity of OAA and MADS is the same.

Qimei Cui et al. [2017] predicted the main dilemma among heterogeneous, ultra-dense, distributed unlicensed spectrum networks in [13]. It's a metric for effective ability that quantifies maximum data rate accuracy while avoiding QoS violations. Power management, admission control, and resource distribution are all possible with the non-trivial creation over heterogeneous ultra-dense networks with potential applications. When compared to current technology, the samples provide significant benefits.

Chun-Hung Liu et al. [2015] consider m-tier HetNet with separate Poisson Point Process (PPPs) in [14]. Each tier APs simultaneously access licensed spectrum, while K^{th} tier APs use the Carrier Sense Multiple Access/Collision Avoidance (CSMA/CA) protocol to assign unlicensed spectrum to APs. The distribution of cell load is first examined as it is cast off to obtain mean cell load, with APs dependent associated probability in each rank. It distinguishes void APs probability in each tier in relation to APs channel

access probability in unlicensed spectrum over densely deployed HetNet. For channel gain/AP weight models, a new method is established to obtain tight lower bounds on AP spectral efficiencies over licensed and unlicensed spectra. APs throughput and per-user network throughput are projected to increase, correspondingly, centralized/decentralized traffic management systems. These are shown to have the highest per-user connection throughput capability.

Xiaoli Chu et al. [2014] looked at the problems and opportunities of HetNet and coexisting Wi-Fi sharing unlicensed spectrum in [15]. To build unlicensed spectrum over Wi-Fi networks, the LTE/ Long Term Evolution Advanced (LTE-A) architecture with small cells was introduced. When both Wi-Fi and LTE/LTE-A are transmitting in the same unlicensed spectrum, the ABS/interference avoidance method helps to reduce interference. The findings revealed that interference avoidance schemes and ABS mechanism use, small cell networks, and heterogeneity increase capacity with unlicensed spectrum using Wi-Fi systems without affecting Wi-Fi output.

Ming Li et al. [2016] looked into the EE, Spectral Efficiency (SE), and Deterministic Equivalent (DE) crises in ultra dense networks in [16]. The coefficients were used in a cooperative Nash equilibrium with an adaptable utility function, where the EE problem is transformed into a power-coordination crisis. Circuit power usage and calming capital expenditure (CapEx) variables are used to achieve the best interference-aware power-coordination solutions. It was thought that a simpler method would reduce the difficulty of signalling overhead. As a result, the cooperative Nash coordination protocol reached Pareto-optimal equilibrium. Not only does the proposed approach converge iterations, but it also achieves a better trade-off between SE, EE, and DE. The efficacy of this method is demonstrated by the simplified algorithm power-coordination efficiency.

Yuxing Mao et al. [17] suggested a negotiating game that, despite hierarchical wireless sensor network (HWSN), found a spectrum-sharing scheme. It allows HWSNs to work with a variety of spectra requirements. When it comes to trade and fairness performance probabilities, HWSN's load of less than 1.5 would be the better choice. Ramona Trestian et al. [18] propose heterogeneous multi-user-multi-provider technology, in which users can freely move from one RAT/SP to another. The mutual existence of SPs and users is noted here. However, just as service providers want to maximise their income by attracting clients, consumers seek the best value for the amount they pay. Gaming theory is widely used to investigate interactions between rational decision makers, and it aids network selection strategies.

3 Proposed Work

This section discusses the proposed methodology for modelling a 3D HetNet model.

3.1 3D Heterogeneous Network System Model

In a 3D HetNet system, a Multi-tier 3D HetNet cellular model is planned first, as shown in Fig. 1 "M" is the M-tier of BSs in this system model, with M = 3. The device is made up of a Multi-Tier of randomly positioned BS with a density of m and a transmit capacity of P_m, where m = 1, 2,..m. The base stations are distributed in 3D space to meet the minimum inter-BS distance constraint (d_{min}).

To model 3D PPP, which is an effective process for modelling a 3D pattern of randomly distributed BS, with the minimum permitted distance between any points being referred to as the multi-core distance. Users of the application are assumed to be placed using PPP, in which each user is expected to use nearby BS from any tier 'm'. Figs. 1 and 4 depicts a 3-Tier 3-D model with M = 3 and a length of L = 100 m. Allow d_i to be the distance between the given users u_i and the nearest BS transmitter.
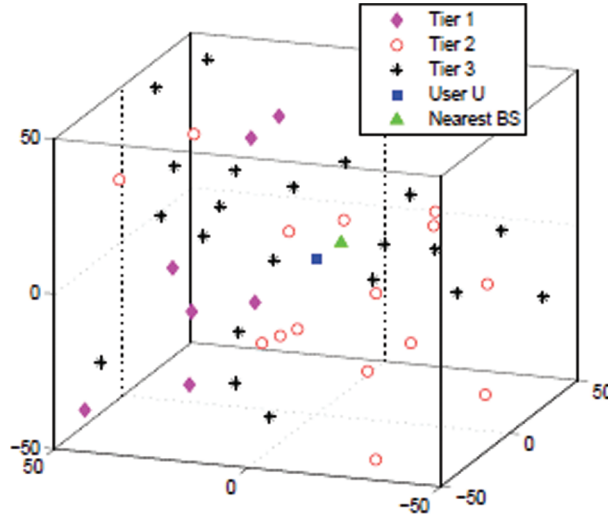
Figure 1: 3D multi-tier HetNet model

The Eq. (1) given below demonstrates the loss of signal received power to user u_i,

$$PL\ (d_i)\ =\ PL\ (1)\ +\ 10\ \alpha\ \log 10\ (d_i)\ +\ 10\ \log 10\ (\gamma,\ d_i) \tag{1}$$

where,

PL (1) - path-attenuation (1 meter); α - path-loss exponent coefficient, γ - attenuation parameter;

Based on the above value, the signal attenuation can be presented as given below Eq. (2),

$$PL\ (d_i)\ =\ Ad_i^{\ -(\alpha+1)} \tag{2}$$

where, $A = 1\ /\ (\gamma^{10PL\ (1)/10})$;

Consider a consumer who is linked to the C_n connected network's roots. Allow C_n to be the user's closest base station. Channel fading gains are common in the connection between the co-ordinator, target user, and base station. BS uses the same carrier frequency at the same time in this planned multi-tier 3D. In the same way, the SNIR is calculated using Eqs. (3) and (4). As the likelihood of transmission decreases, the SINR value rises. In the M-Tier HetNet model, SINR is often used to determine the precise distance between transmitter and receiver.

$$SINR\ =\frac{P_t HA_r^{-}(\alpha+1)}{I_u\ +\ \sigma_n^2} \tag{3}$$

where,

$$I_u = \sum_{i\,\epsilon\,\phi\{C_0\}} qP_i G_i Al_i^{\alpha+1} \tag{4}$$

$H = \|h\|^2$; $G_i = \|g_i\|^2$ is squared magnitude operator;

l_i - distance between base station and user ; q - Transmit probability; P_i (P_t) - Transmit power of BS

σ^2- Additive white Gaussian noise power.

Based on the PPP model with density of multi-tier 3D model, $\beta_m = \sum_{k=1}^{k} \lambda_k$

In this model, every parent node is randomly associated and node does not retain only, when there exists another node within distance d_{min}. Based on the correlation between nodes retaining event and the probability of anode are provided as in Eq. (5):

$$\tau = \left[1 - exp\left(-\frac{4}{3} \pi\lambda_p d_{min}^3\right)\right]/\left[\frac{4}{3} \pi\lambda_p d_{min}^3\right)\right] \tag{5}$$

The density λ is given by weighting τ with λ_p. λ_p specifies the PPP density. According to this, probability of d_i is greater than distance d; where d is that there is no existence of BS in a certain region. By using this PPP density function, the approximation is given in Eq. (6),

$$P_r\{d < d_j\} \approx \sum_{v=0}^{N_p}\left\{\frac{(1-T)^v\left(\dfrac{4\frac{4}{3}\pi\lambda P^{d^3}min}{3}\right)}{V!}\right\} exp\, exp - \frac{4}{3}\left(\pi\lambda P^{d^3}min\right) \tag{6}$$

where, $N_p = [\lambda_p R^3]$. N_p is the side length of the system model with PPP density.

Therefore, the cumulative distributive function of d_i, is given as in Eq. (7) below:

$$f(d_1) = exp\left\{\left(\frac{4}{3}\pi\lambda_p r_1^3\right)4\pi\lambda_p r_1^2 + \sum_{v=1}^{N_p}\{(1-T)^v\left[\frac{\frac{4}{3}\pi\lambda Pr_1^{3v+2}}{V!} - \frac{3r_1^{3v}-1}{(v-1)!}\right]\}\right\} \tag{7}$$

Received interference signal degrades average device output due to concurrent transmission from various cells. A novel cross-tier interference management model is proposed to remove the cross-interference problem.

3.2 Cross-Tier Interference

Cross tier interference occurs when one tier interferes with another tier in an M-tier communication scheme. By controlling inter-cell interference and promoting frequency reuse, this section discusses interference synchronisation between licensed and unlicensed spectrum. The concept of a "Completely Blank Subframe" (CBS) was used. Reduced interference is achieved by not transferring such sub-frames to other cells. However, fully halting signal transmission has a number of drawbacks. As a consequence, it is recommended that signals be transmitted at a very low power level, if not absolutely stopped. The 'Almost Blank Subframe (ABS)' is a subframe with very low signal strength. As a result, no large amounts of data are transmitted, but channel controlling strategies based on spectrum allocation with extremely low power are considered. In general, licensed and unlicensed spectrum uses this "ABS" to provide smart spectrum allocation between interfering cells and improve load balancing in the M-Tier 3D HetNet model. BS typically uses a non-overlapping ABS configuration to coordinate data transmission over a standard spectrum. When a macro cell base station configures an ABS sub-frame, the femto-cell base station transmits normally, and femto-cell users receive data without macro cell base station intervention. Similarly, macro cell users will obtain data from macro base station when femto base station configures an almost-blank subframe. Connecting fibre can be used to negotiate almost-blank subframe configurations between macro and femto BSs.

Cross-tier interference between macro and femto base stations is done using time-division duplexing in a multi-tier 3D scheme. The signal-to-noise ratio (SNR) of received signals is measured as follows:

$$SNR^{t,f}(m) = \frac{P_p^2 ||H||^2}{\sigma_n^2} \tag{8}$$

$$SNR^{t,f}(f) = \frac{P_s^2 ||G||^2}{\sigma_n^2} \tag{9}$$

where,

σ_n^2 - noise variance; p - transmit power; $SNR^{t,f}(m)$ - signal to noise ratio in macro cell;

$SNR^{t,f}(f)$ - signal to noise ratio in femtocell; H and G – Rayleigh fading channel

In order to focus on spectral efficiency, every BS schedules users with higher SNR. Therefore, for each 'ABS' femto and macro BS schedules maximum users as per Eqs. (10) and (11):

$$SNR^{t,f}(m_{max}) = \max SNR^{t,f}(m) \tag{10}$$

$$SNR^{t,f}(f_{max}) = \max SNR^{t,f}(f) \tag{11}$$

The most significant drawback of cross-tier interference in multi-tier 3D HetNet is that interfering BS cannot reach the spectrum at the same time. Any base station is only allowed to use non-nearly blank sub-frames, which decreases EE. EE - based CA is used to address this constraint.

3.3 Carrier Aggregation

CA is a technology that combines/merges two or more carriers into a single data channel in order to maximise data bandwidth. This segment discusses using carrier aggregation to gain access to available spectrum in order to increase EE. CA plays a critical role in ensuring that service providers have the greatest possible versatility in using the entire spectrum. HetNet allows Wi-Fi and LTE to provide much higher throughput by partitioning the available spectrum into multi-tiers [19]. Asymmetric aggregation (using a different amount of bandwidth on the uplink and downlink) provides more flexibility and solves the issue of downlink traffic to increase energy efficiency. Certain aggregation types are Intra-band over non-adjacent channels, Intra-band over adjacent channels and Inter-band (1.9 GHz, 700 MHz). Owing to technical concerns, interband technology is not currently being investigated. Integrating the unlicensed and licensed spectrum must be investigated to resolve certain technical problems, as seen in the following section.

3.4 Integrating Licensed and Unlicensed Spectrum

In order to provide enhanced packet data gateway and trusted wireless access gateway, the convergence of unlicensed and licensed spectrum is critical. In general, 3 GGP technical requirements are used to incorporate licensed and unlicensed band technologies as a starting point. Unlicensed network convergence technologies, such as Wi-Fi, are largely emerging as a precursor to the evolution of mobile networks for use with conventional licensed cellular networks. Unlicensed 5 GHz solutions, in comparison to licensed spectrum allocation, enable service providers to sell more than 450 MHz of unlicensed spectrum [20].

The suggested solution creates the link by merging Wi-Fi with the LTE core network. A trusted non-3GGP IP access interface is used here to incorporate unlicensed spectrum using a trusted wireless access gateway. This is commonly used to move 4G data to Wi-Fi [21]. After that, an untrusted non-3GGP IP access solution employs an improved packet data gateway to collaborate with the 3GPP core network

through a packet data network gateway. This strategy is widely used to maximise energy efficiency by offering indoor Wi-Fi coverage. Furthermore, these solutions have the downside of not allowing for proper carrier convergence of unlicensed and licensed spectrum. The next segment goes into how to deploy CA for LTE-Wi-Fi integration.

3.4.1 LTE - Wi-Fi Integration through HetNets

A CA mode for LTE and Wi-Fi integration via M-Tier 3D HetNets is expected. Wi-Fi and LTE networks are initially coordinated [22]. In the event that spectrum is available, LTE borrows it from the Wi-Fi band and distributes it to LTE Advanced (LTE-A) for aggregation. In an organisational environment, for example, an LTE-A base station works with a Wi-Fi access point to request Wi-Fi channels in a contention-free mode, and thus appears as a Wi-Fi user [23]. LTE-A base stations use the borrowed channel as part of the LTE-A spectrum. This communication between the BSS and the AP takes place over the air interface or the wired interface, allowing the BSS to function as a Wi-Fi station. Another choice is for the integrated BSs-AP to use Wi-Fi spectrum for LTE-A transmission based on the demand for both Wi-Fi and LTE-A transmission. This is theoretically a technique that will cover 5G in the future while also lowering energy consumption. The bandwidth requirements and Wi-Fi spectrum availability are needed for measuring LTE-A-Wi-Fi aggregation mode. As a result, before going live, Wi-Fi spectrum connectivity should be considered as part of the LTE-A/Wi-Fi interference study. The implementation of LTE-Wi-Fi dependent carrier aggregation is discussed.

3.4.2 LTE and Wi-Fi Coexistence using Carrier Aggregation

802.11 Distributed Coordination Function (DCF) is a carrier sensing protocol with a four-way handshake that takes advantage of throughput during collision avoidance. For each node, CSMA/CA is used. The node attempting transmission must satisfy certain carrier sensing mechanisms while the medium is idle. There is no active transmission if the channel is idle. If a channel is busy or congested after a good transmission, the station monitors it until it becomes idle during the DCF cycle. The back off counter is chosen uniformly, with values starting at 0 and W_0 (minimum contention window).In terms of the network's collision nature, it's a control method for lowest priority. Each failed transmission caused by a packet collision raises the back-off stage by one, and the node counts the back-off value. When no more transmissions are detected, the node decrements the counter ('s') to the back-off slot. If a busy channel is detected with countdown, counting is paused, and nodes continue to sense the busy channel until it is idle.

When the counter reaches zero, the node begins sending packets over LTE and Wi-Fi. If a node does not complete its countdown to 0, the current round holds the back-off value and the next round begins. The value is reset to 0 when the transmission is effective [24]. If the transmission fails, the node drops the packet and resets the off value to 0. After good receipt of a unicast transmission, the receiver transmits an acknowledgment frame (ACK). The following is the energy calculation:

a) Clear channel assessment (CCA) is performed by LTE-Licensed Assisted Access (LTE-LAA) using 'energy detect' to sense the channel for the defer duration (Td). Td is determined by the priority class number. For preamble detection, there is no carrier sensing in (LTE-LAA), as there is in Wi-Fi. In LTE-LAA, there are two situations to test CA. In one, if the channel is sensed idle, current contention does not carry out immediate successful transmission, while LTE-LAA nodes do. If the channel is sensed to be busy in the future, it reverts to the available extended CCA. Extended Clear Channel Assessment (eCCA) detects and defers Td until the channel is idle. Later LTE-LAA performs a distributed coordination function as in Fig. 2.

b) LTE-LAA-coordinated four-channel access priority class [25], with separate maximum and minimum CWS.
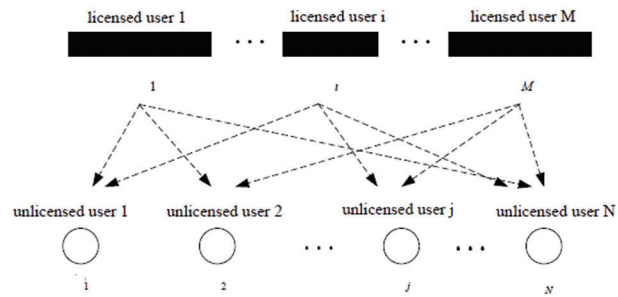
Figure 2: LTE-LAA contention window size

c) When a collision occurs, the Contention Window Size (CWS), i.e., [0, 2iW01-1], is used to calculate the back-off number for re-transmission. The letter I stands for the re-transmission process, which is used to select CWS. If I reaches the maximum re-transmission stage 'm/,' where it remains at the maximum window size for 'el,' where 'er' is the limit after hitting m/, I is reset to 0, and 'el' is chosen from value ranges of 1, 2, 3,… 8.

d) When the LTE-LAA operator obtains channel access, it enables packet transmission for the next transmission opportunity period up to 10 ms when there is no co-existence node, and up to 8 ms when there is no co-existence node for simulation purposes.

e) LTE-minimal LAA's data transmission consists of a single sub-frame (i.e., 1 ms), with LTE-LAA traversing a single sub-frame for a 0.5 ms slot.

f) If data is in the LTE-LAA buffer after the maximum transmission time, it must perform eCCA to reach the channels.

The smallest radio resource unit in LTE is the resource block, which is equal to 180 kHz bandwidth during the transmission time sub-frame interval. Each 180 kHz bandwidth resource block has 12 sub-carriers, 14 Orthogonal Frequency Division Multiplexing (OFDM) symbols, and 168 resource elements. Any resource element or symbol in a resource block carries 2, 4, or 6 BPS in coding schemes like 16-Quadrature Amplitude Modulation (QAM), 64-QAM, Quadrature Phase Shift Keying (QPSK), and modulation. The LTE-LAA system, which has a bandwidth of 20 MHz, will have about 100 resource blocks. There are 14 OFDM symbols in each sub-frame; with 1–3 being downlink control channels and 11 being downlink shared channels. LTE-LAA slot boundaries transmission commences at 0.5 ms LTE slots for one sub frame. Before commencing the next transmission, it has to transmit the reservation signal for channel reservation [26]. After transmission period, receiver transmits ACK via licensed band, if those signals are decoded successfully.

4 Results and Discussions

Fig. 1 demonstrates the position of small cells in 3D M-Tier HetNets, and this helps to analyse the energy consumption and coverage output improvement with small cell density deployment. The distributions of macro-cells, pico-cells, and femto-cells are all done separately using the Poisson point technique. The simulation is run, and the results of the numerical computation are evaluated after several iterations. The criteria considered for Wi-Fi and LTE evaluations are shown in Tab. 1:

Table 1: LTE & Wi-Fi simulation parameters

Parameters	Value
LTE carrier frequency	2200 MHz
Wi-Fi carrier frequency	2600 MHz
LTE density	$4/km^3$
Wi-Fi density	$350/km^3$
LTE transmission power	40 W
Wi-Fi transmission power	1 W

This data aggregation tree structure in Fig. 3 helps in data transmission at random in the available spectrum.
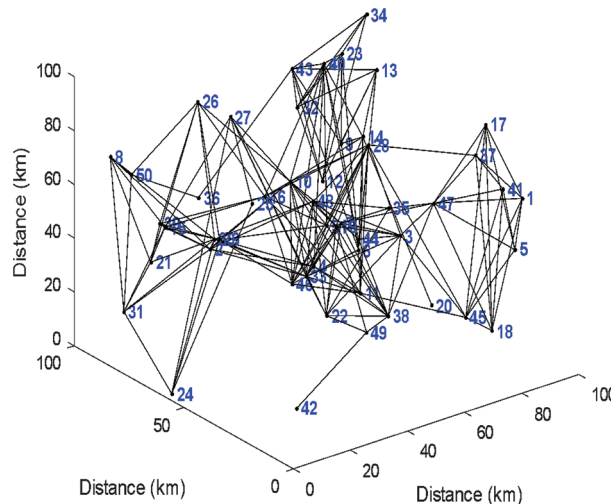
Figure 3: Tree structure plot for data aggregation in femto, pico and macro cells

Femto, pico, and macro cells are randomly placed in Fig. 4. The Fig. 5 depicts the convergence probability *vs*. SINR threshold T decibel (dB) for different tier counts. Convergence probability is used to indicate interference from smaller cells, which degrades HetNets efficiency. In a multi-tier architecture, increasing the number of users results in gradual gains in M-tier and improves convergence.

Fig. 6 portrays a graphical depiction of the available users' energy efficiency. Small cell deployment enhances energy efficiency; but, as small cell density grows, benefit saturates. The power spectrum of the input carrier signal is estimated. However, the static power of micro base stations contributes to macro deployment; Heterogeneous region power consumption is often higher than pure macro deployment. The Pico BS power consumption is lower than macro BS due to structural variations between the two.

In a MSCA 3-Tier HetNet, Fig. 7 portrays the Almost Blank Frames. The usable spectrum in the LTE coverage area is investigated by comparing Almost Blank Subframes (ABS) 1 and 2 (an Inter-cell Interference coordination mechanism present in LTE).

Fig. 8 shows the packet success rate evaluation. Packet Success Rate (PSR) evaluation is dependent on received power (P) and SINR.
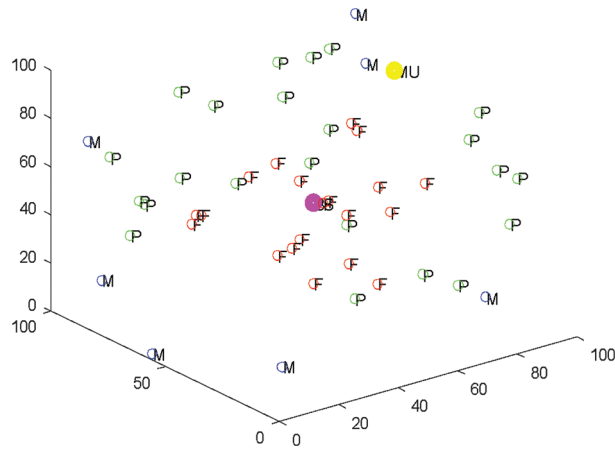
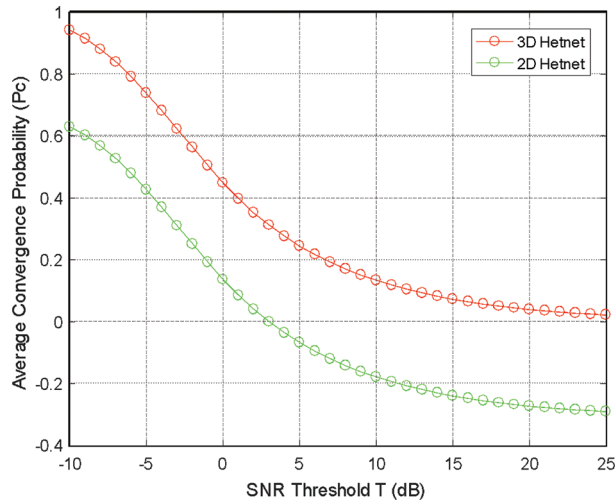**Figure 4:** Random femto, pico and macro cells

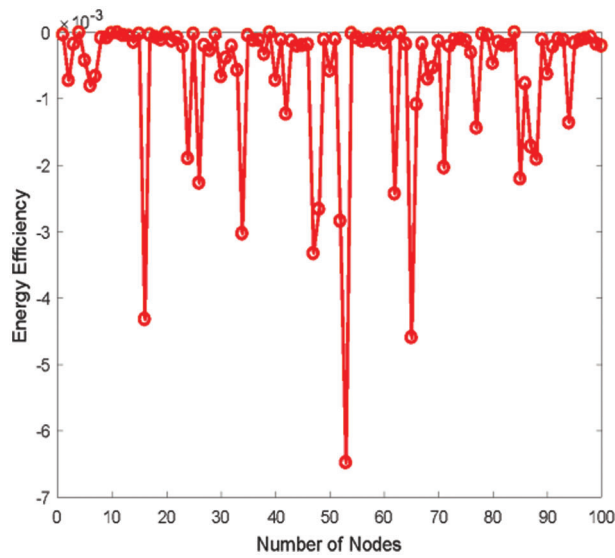**Figure 5:** Convergence probability with respect to SNR between 2D and 3D

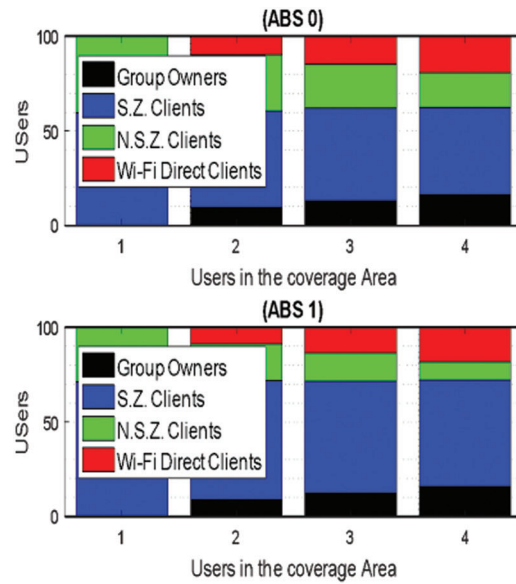**Figure 6:** Estimation of energy efficiency of available users

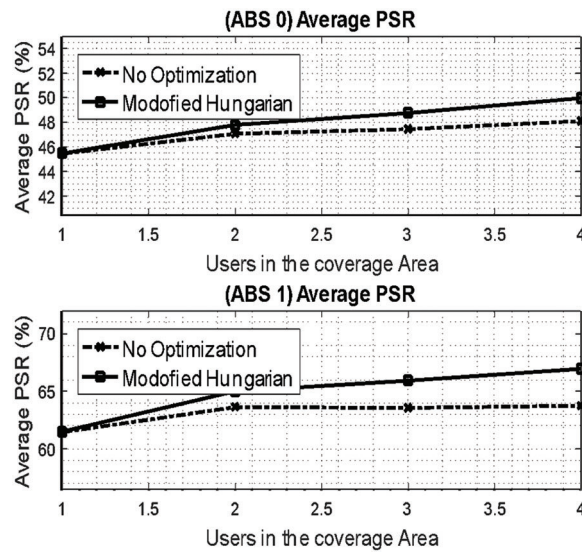**Figure 7:** Number of users *vs.* coverage region

Figure 8: Packet success rate evaluation

The throughput and CDF analysis in the HetNet setting are depicted in Figs. 9–11. CDF is specifically used to determine the SINR in both small cells and macro cells in users. The CDF is also used to measure the average BER. It must achieve CDF scheduling throughput.

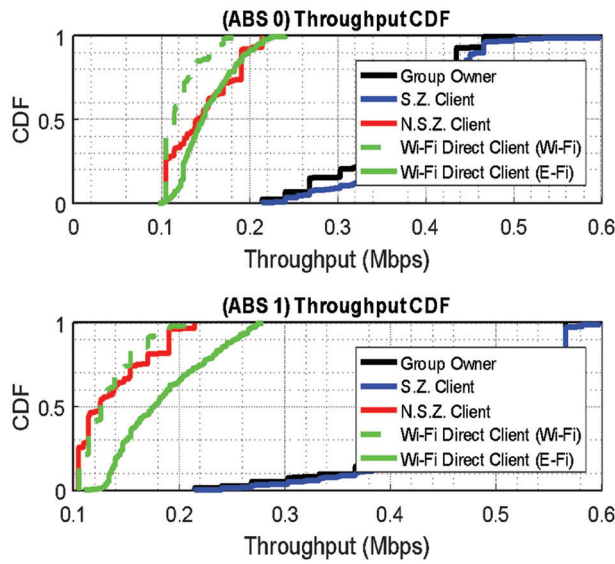**Figure 9:** Average throughput *vs.* users in the coverage area

Figure 10: Cumulative distribution function (CDF) *vs.* throughput (in Mbps)

Assume that LTE-LAA/Wi-Fi is a co-channel with a buffering condition to ensure 3GPP reliability. Then, downlink (DL) transmission (AP/client) shows that APs are involved in contention. Assume that w is the likelihood of Wi-Fi connectivity for each time slot. As a result, as shown in Eq. (12) below, the network has the lowest collision probability with the least transmission and the others remain in the station:

$$P_w = 1 - (1 - \tau_w)^{n-1}(1 - \tau_l)^{n_l} \tag{12}$$

where P_w - coupling of both Wi-Fi/LTE-LAA nodes through τ_w and τ_l.
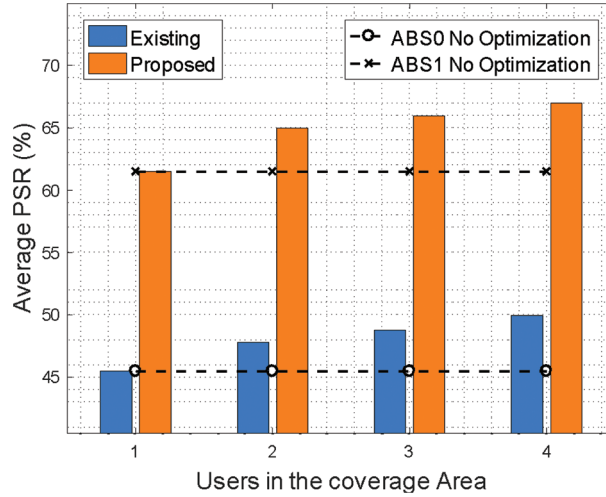
Figure 11: Average throughput *vs*. users in the coverage area

Similarly, collision probability amongst LTE-LAA with remaining station is given in Eq. (13):

$$P_l = 1 - (1 - \tau_l)^{n-1} \ ((1 - \tau_w)^{n_l} \tag{13}$$

where, P_l depends on both LTE-LAA/Wi-Fi via τ_w and τ_l.

$$P_{transmission} = 1 - (1 - \tau_w)^{n_l} \tag{14}$$

Wi-Fi transmission probability depends on contention parameters related to both Wi-Fi and LTE-LAA via τ_w. It is the probability that one station can transmit a packet based on the provided time slot. Similarly, LTE-LAA transmission probability is given by Eq. (15):

$$P_{transmission} = 1 - (1 - \tau_l)^n \tag{15}$$

In order to establish a successful Wi-Fi transmission, one station has to make an attempt to establish transmission to the other users also as in Eq. (16):

$$P_{successful} = \frac{\tau_w (1 - \tau_w)^{n_l - 1}}{P_{transmission}} \tag{16}$$

As well, LTE-LAA successful transmission probability is computed as Eq. (17):

$$P_{successful} LTE = \frac{\tau_l (1 - \tau_l)^{n_l - 1}}{P\_transmission} \tag{17}$$

After performing successful transmission, Wi-Fi throughput is calculated using Eq. (18):

$$Throughput_{WiFi} = \frac{P_{transmission} P_{successful} (1 - P_{transmission}) P\_size}{T_E} R_w \tag{18}$$

where

$P_{transmission} P_{successful} (1 - P_{transmission})$ - Probability of Wi-Fi transmitting packet in single time slot,

R_w - Wi-Fi data rate in physical layer. As well, LTE-LAA throughput is calculated as in Eq. (19):

$$Throughputt_{LTE\,LAA} = \frac{P_{transmission}P_{successful}LTE\,(1 - P_{transmission})\frac{13}{14}T_D}{T_E}R_1 \qquad (19)$$

where $\frac{13}{14}T_D$ is Data transmission

Fig. 12 shows the transmission time required for establishing communication between the network users in the HetNet environment.
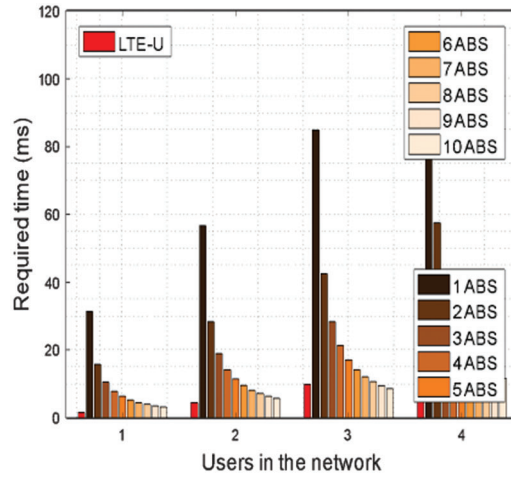

Figure 12: Transmission time *vs*. network users

4.1 Energy Metrics

Following the evaluation of LTE-LAA and Wi-Fi throughput, energy efficiency must be assessed among the nodes. Total energy consumption in a multi-tier HetNet is calculated using the total operating power TP_{op} and total embodied power TP_{em} of all base stations in the network structure provided, as shown in Eqs. (20) and (21):

$$TP_{op} = N_{macro}\,*TP_{em} + M_{relay\,node}*TP_{op}^{relay\,node} + N_{micro}*TP_{op}^{micro} \qquad (20)$$

$$E_{Em}^{total} = N_{macro}*E_{Em}^{macro} + M_{relaynode}*E_{Em}^{relay\,node} + N_{micro}*E_{Em}^{micro} \qquad (21)$$

where

N_{macro} - Total number of macro base station in a network;

N_{micro}- Total number of micro base station in network;

$M_{relaynode}$ - Total number of relay node base stations in a network.

While E_{Em} macro - Energy/macro base station; E_{Em} micro - Energy/micro base station;

E_{Em} relay node - Energy/relay node base station;

Energy efficiency or energy reduction gain (%) is derived from the Eq. (22). It is depicted as the ratio of total energy consumption for baseline network of HetNet as in Eq. (21):

$$\text{Energy efficiency } = \left(1 - \frac{\left(E_{op}^{total} + E_{Em}^{total} \right)_{Multitier\,HetNet}}{\left(E_{op}^{total} + E_{Em}^{total} \right)_{baseline}} \right) * 100\% \tag{22}$$

Where E_{op}^{total} - Operational energy is equivalent to operational power per second period.

5 Conclusion

When the field of wireless communication grows, so does the need for data transmission, which necessitates a vast amount of bandwidth. Wi-Fi, by using unlicensed spectrum allocation, provides a cost-effective way to meet the need for high data availability. Due to spectral performance and coverage area limits, the concept of merging Wi-Fi and LTE network connectivity has been suggested. This work focuses on the design of a 3D multi-tier HetNet for evaluating various factors such as energy, Wi-Fi and LTE coexistence, throughput, and so on, using this as a benchmark. These Wi-Fi upgrades provide consumers with higher throughput and offload solutions, as well as cost savings, when using unlicensed spectrum.

The SNIR was investigated using a M-Tier 3D HetNet model that analysed cumulative Femto-tier and Pico-tier interference. Following that, the channel allocation scheme is examined in order to calculate device channel throughput for multiple tiers. In addition, the problem of M-Tier 3D HetNet in terms of throughput and energy metrics, as well as LTE and Wi-Fi coexistence using MSCA, was formulated. Simulations at the system level were run in the HetNet setting, revealing a substantial increase in energy efficiency. The discovery aids in the creation of effective M-Tier 3D HetNets for improving energy efficiency. The key aim of HetNet optimization is to increase energy efficiency in the planning, implementation, network management, and service stages of the ecosystem for economic sustainability. This paper investigates the recent effort on energy awareness using a variety of deployments, including micro, macro, and picocells. In future, this work can be extended by employing 3D M-Tier HetNet using improved form of Multistream Carrier Aggregation and analysing its application in healthcare sector.

Conflicts of Interest: The authors declare that they have no conflicts of interest to report regarding the present study.

References

[1] M. K. Hasan, A. F. Ismail, A. H. Abdalla, K. Abdullah and H. A. M. Ramli, "Performance analysis of interference coordination techniques in heterogeneous network," *Research Journal of Applied Sciences, Engineering and Technology*, vol. 7, no. 8, pp. 1536–1550, 2014.

[2] J. G. Andrews, S. Buzzi, W. Choi, S. Hanly, A. Lozano *et al.,* "What will 5G be?," *IEEE JSAC Special Issue on 5G Wireless Communication Systems*, vol. 32, no. 6, pp. 1065–1082, 2014.

[3] B. Zhuang, D. Guo and M. L. Honig, "Traffic-driven spectrum allocation in heterogeneous networks," *IEEE Journal on Selected Areas in Communications*, vol. 33, no. 10, pp. 2027–2038, 2015.

[4] X. Chu, D. Lopez-Perez, Y. Yang and F. Gunnarsson, "Heterogeneous cellular networks: Theory, simulation and deployment," 1st ed., New York, USA: Cambridge University Press, pp. 1–494, 2013.

[5] M. Charitos and G. Kalivas, "Heterogeneous hybrid vehicular WiMAX-Wi-Fi network for in-tunnel surveillance implementations," *IEEE International Conference on Communications*, vol. 33, pp. 6386–6390, 2013.

[6] S. Dimatteo, H. Pan, B. Han and V. O. K. Li, "Cellular traffic offloading through WiFi networks," *IEEE International Conference on Mobile Ad Hoc and Sensor System*, vol. 11, pp. 192–201, 2011.

[7] S. Wang, W. Guo and M. McDonnell, "Downlink interference estimation without feedback for heterogeneous network interference avoidance," *IEEE International Conference on Telecommunications*, vol. 14, pp. 82–87, 2014.

[8] I. Hwang, B. Song and S. S. Soliman, "A holistic view on hyper-dense heterogeneous and small cell networks," *IEEE Communications Magazine*, vol. 51, no. 6, pp. 20–27, 2013.

[9] C. X. Wang, F. Haider, X. Gao, X. H. You, Y. Yang *et al.,* "Cellular architecture and key technologies for 5G wireless communication networks," *IEEE Communications Magazine*, vol. 52, no. 2, pp. 122–130, 2014.

[10] C. H. Liu and H. C. Tsai, "Decentralized traffic management for heterogeneous networks with opportunistic unlicensed spectrum sharing," *IEEE International Workshop on Spatial Stochastic Models for Wireless Networks*, vol. 17, pp. 1–6, 2017.

[11] Z. Zhou, D. Guo and M. L. Honig, "Allocation of licensed and unlicensed spectrum in heterogeneous networks," *IEEE Australian Communications Theory Workshop*, vol. 16, pp. 59–64, 2016.

[12] M. Ali, S. Qaisar, M. Naeem, J. J. P. C. Rodrigues and F. Qamar, "Resource allocation for licensed and unlicensed spectrum in 5G heterogeneous networks," *Wiley Transactions on Emerging Telecommunications Technologies*, vol. 29, no. 6, pp. 1–15, 2018.

[13] Q. Cui, Y. Gu, W. Ni and X. Zhang, "Preserving reliability to heterogeneous ultra-dense distributed networks in unlicensed spectrum," *IEEE Communications Magazine*, vol. 56, no. 6, pp. 72–78, 2018.

[14] C. H. Liu and H. C. Tsai, "Traffic management for heterogeneous networks with opportunistic unlicensed spectrum sharing," *IEEE Transactions on Wireless Communications*, vol. 16, no. 9, pp. 5717–5731, 2017.

[15] H. Zhang, X. Chu, W. Guo and S. Wang, "Coexistence of Wi-Fi and heterogeneous small cell networks sharing unlicensed spectrum," *IEEE Communications Magazine*, vol. 53, no. 3, pp. 158–164, 2012.

[16] M. Li, P. Chen and S. Gao, "Cooperative game-based energy efficiency management over ultra-dense wireless cellular networks," *MDPI Sensors*, vol. 16, no. 9, pp. 1–22, 2016.

[17] Y. Mao, T. Cheng, H. Zhao and N. Shen, "A strategic bargaining game for a spectrum sharing scheme in cognitive radio-based heterogeneous wireless sensor networks," *MDPISensors*, vol. 17, no. 2737, pp. 1–18, 2017.

[18] R. Trestian, O. Ormond and G. M. Muntean, "Game theory-based network selection: Solutions and challenges," *IEEE Communications Surveys & Tutorials*, vol. 14, no. 4, pp. 1212–1231, 2012.

[19] C. H. Liu and H. C. Tsai, "On the limits of coexisting coverage and capacity in multi-RAT Heterogeneous networks," *IEEE Transaction on Wireless Communications*, vol. 16, no. 5, pp. 3086–3101, 2017.

[20] Q. Chen, G. Yu, H. Shan, A. Maaref, G. Y. Li *et al.,* "Cellular meets WiFi: Traffic offloading or resource sharing?," *IEEE Transactions on Wireless Communications*, vol. 15, no. 5, pp. 3354–3367, 2016.

[21] F. Liu, E. Bala, E. Erkip, M. C. Beluri and R. Yang, "Small-cell traffic balancing over licensed and unlicensed bands," *IEEE Transactions on Vehicular Technology*, vol. 64, no. 12, pp. 5850–5865, 2013.

[22] A. Bhorkar, C. Ibars and P. Zong, "Performance analysis of LTE and WiFi in unlicensed band using stochastic geometry," *IEEE International Symposium on Personal, Indoor and Mobile Radio Communications*, vol. 15257394, pp. 1310–1314, 2015.

[23] C. H. Liu and L. C. Wang, "Modeling and analysis of coexisting multiple radio access technologies in heterogeneous wireless networks," *IEEE International Conference on Computing, Networking and Communications*, vol. 15872138, pp. 1–5, 2016.

[24] Q. Cui, Y. Shi, X. Tao and P. Zhang, "A unified protocol stack solution for LTE and WLAN in future mobile converged networks," *IEEE Wireless Communication*, vol. 21, no. 6, pp. 24–33, 2014.

[25] C. H. Liu and K. L. Fong, "Fundamentals of the downlink green coverage and energy efficiency in heterogeneous networks," *IEEE Journal on Selected Areas in Communications*, vol. 34, no. 12, pp. 3271–3287, 2016.

[26] P. Xia, C. H. Liu and J. G. Andrews, "Downlink coordinated multipoint with overhead modeling in Heterogeneous cellular networks," *IEEE Transactions on Wireless Communications*, vol. 12, no. 8, pp. 4025–4037, 2013.